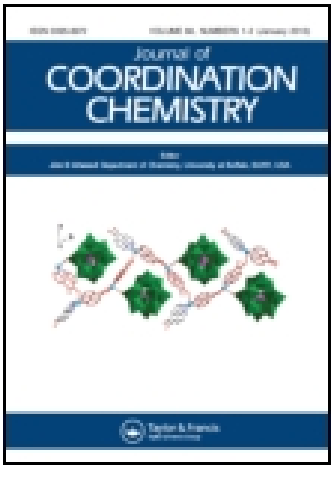

Journal of Coordination Chemistry
Publication details, including instructions for authors and subscription information:
http://www.tandfonline.com/loi/gcoo20

NMR and kinetic studies of the interactions of $[Au(cis\text{-}DACH)Cl_2]Cl$ and $[Au(cis\text{-}DACH)_2]Cl_3$ with potassium cyanide in aqueous solution

Adam A.A. Seliman[a], Muhammad Altaf[a], Abdel-Nasser Kawde[a], Mohammed I.M. Wazeer[a] & Anvarhusein A. Isab[a]
[a] Department of Chemistry, King Fahd University of Petroleum and Minerals, Dhahran, Saudi Arabia
Accepted author version posted online: 13 Oct 2014.Published online: 29 Oct 2014.

To cite this article: Adam A.A. Seliman, Muhammad Altaf, Abdel-Nasser Kawde, Mohammed I.M. Wazeer & Anvarhusein A. Isab (2014) NMR and kinetic studies of the interactions of $[Au(cis\text{-}DACH)Cl_2]Cl$ and $[Au(cis\text{-}DACH)_2]Cl_3$ with potassium cyanide in aqueous solution, Journal of Coordination Chemistry, 67:21, 3431-3443, DOI: 10.1080/00958972.2014.971020

To link to this article: http://dx.doi.org/10.1080/00958972.2014.971020

Journal of Coordination Chemistry, 2014
Vol. 67, No. 21, 3431–3443, http://dx.doi.org/10.1080/00958972.2014.971020

NMR and kinetic studies of the interactions of [Au(*cis*-DACH)Cl_2]Cl and [Au(*cis*-DACH)$_2$]Cl_3 with potassium cyanide in aqueous solution

ADAM A.A. SELIMAN, MUHAMMAD ALTAF, ABDEL-NASSER KAWDE, MOHAMMED I.M. WAZEER and ANVARHUSEIN A. ISAB*

Department of Chemistry, King Fahd University of Petroleum and Minerals, Dhahran, Saudi Arabia

(*Received 7 April 2014; accepted 10 September 2014*)

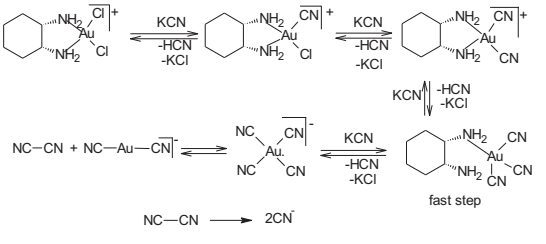

The interactions of [Au(*cis*-DACH)Cl_2]Cl and [Au(*cis*-DACH)$_2$]Cl_3 [where *cis*-DACH is *cis*-1,2-diaminocyclohexane] with enriched KCN were carried out in CD_3OD and D_2O, respectively. The reaction pathways of these complexes were studied by ^{1}H, ^{13}C, ^{15}N NMR, UV spectrophotometry, and electrochemistry. The kinetic data for the reaction of cyanide with [Au(*cis*-DACH)$_2$]Cl_3 are $k = 18\ M^{-1}s^{-1}$, $\Delta H^{\neq} = 11\ kJ\ M^{-1}$, $\Delta S^{\neq} = -185\ JK^{-1}\ M^{-1}$, and $E_a = 13\ kJ\ M^{-1}$ with square wave voltammetric (SWV) peak +1.35 V, whereas the kinetic data for the reaction of cyanide ion with [Au(*cis*-DACH)Cl_2]Cl are $k = 148\ M^{-1}s^{-1}$, $\Delta H^{\neq} = 39\ kJM^{-1}$, $\Delta S^{\neq} = -80\ JK^{-1}\ M^{-1}$, and $E_a = 42\ kJM^{-1}$ along with SWV peak +0.82 V, indicating much higher reactivity of [Au(*cis*-DACH)Cl_2]Cl toward cyanide than [Au(*cis*-DACH)$_2$]Cl_3. The interaction of these complexes with potassium cyanide resulted in an unstable $[Au(^{13}CN)_4]^-$ species which readily underwent reductive elimination reaction to generate $[Au(^{13}CN)_2]^-$ and cyanogen.

Keywords: [(*cis*-DACH)$AuCl_2$]Cl complex; K^{13}CN; Reductive elimination; Rate constant

1. Introduction

Recently, chemical and biochemical studies of Au(III) complexes containing N-chelating ligands have shown biological activity [1–8]. In addition, a number of other Au(III) complexes with N-chelating ligands have been developed with promising anticancer and cytotoxic activities. Gold(III) complexes have square planar d^8 configuration, which is

*Corresponding author. Email: aisab@kfupm.edu.sa

isoelectronic with Pt in the antitumor agent *cis*-diaminedichloroplatinum(II) (*cisplatin*) and in *cis*-1,2-diaminocyclohexane dichloroplatinum(II) (DACH) complexes. The new gold(III) complexes may be attractive as anticancer drugs to overcome *cisplatin* side effects [2, 9–13].

Al-Maythalony *et al.* investigated the interaction of Au(III)-alkyldiamine complexes with L-histidine and imidazole ligands by ^{1}H, ^{13}C NMR, and UV spectrophotometry, and found that the rate of reaction is dependent on pH [14]. Zhu *et al.* reported the synthesis, structure, and electrochemistry of Au(III) ethylenediamine complexes and their interactions with guanosine-5-phosphate [15]. Sanghvi *et al.* described antitumor properties of five-coordinate gold(III) complexes bearing substituted polypyridyl ligands, and found that [(sec-butyl) phen)$AuCl_3$] has more significant *in vitro* antitumor activity than metallotherapeutic *cisplatin* [16]. Ahmed *et al.* studied histological changes in kidneys and livers of rats due to exposure of [Au(en)Cl_2]Cl [17]. Al-Jaroudi *et al.* described synthesis, characterization, and cytotoxicity of gold(III) complexes with 1,2-diaminocyclohexane and showed the influence of stereochemistry on antitumor activity [18].

Monim-ul-Mehboob *et al.* prepared a series of Au(III)-alkanediamine complexes, with ethylenediamine, propylenediamine, butylenediamine, and N-alkyl substituted ethylenediamine, those were characterized and tested against gastric, prostate, and ovarian cancer cells [19].

The interaction of Au(III) with cyanide has interest in therapeutic values and pharmacological activity, due to the formation of $[Au(CN)_4]^-$, which is unstable in physiological condition and produces $[Au(CN)_2]^-$. Cyanide is naturally produced in the body by oxidation of SCN^- by the enzyme, myeloperoxidase, and released by phagocytic cells [20–22].

The $[Au(CN)_2]^-$ has been extensively used in the treatment of rheumatoid arthritis since the 1920s, while other Au(I) complexes showed activity against malaria and HIV [23, 24].

Canumalla *et al.* described redox and ligand exchange reactions of potential gold(I)- and gold(III)–cyanide metabolites under biomimetic conditions [25]. Yangyuoru *et al.* studied the reduction of auricyanide using glutathione (GSH) as reductant through two intermediates I_{230} and I_{290} [26].

Al-Maythalony *et al.* described ^{1}H, ^{13}C NMR, and UV spectroscopy studies of gold(III)-tetracyanide with L-cysteine, GSH, captopril, L-methionine, and DL-seleno-methioninein aqueous solution [27].

In this paper, we have investigated the interaction of [Au(*cis*-DACH)Cl_2]Cl and [Au(*cis*-DACH)$_2$]Cl_3 with KCN and present some kinetic data.

2. Experimental

2.1. *Chemicals*

$NaAuCl_4 \cdot 2H_2O$, *cis*-DACH ($C_6H_{14}N_2$) were purchased from Sigma–Aldrich, USA, abs. EtOH from Merck, CH_3OD and D_2O were purchased from Alfa-Aesar, KCN, 99.9% enriched $K^{13}CN$ and 99% enriched $K^{13}C^{15}N$ from Cambridge Isotope Lab. Inc. Deionized water with a resistivity of 18.6 MΩ cm^{-1} is used to prepare all solutions. The water is obtained directly from a PURELABs Ultra Laboratory Water Purification System (http://www.water.siemens.com).

2.2. *Spectroscopic techniques*

UV spectral measurements were carried out using a Lambda 200 Perkin Elmer UV–vis spectrophotometer and Cary 100 spectrophotometer from 200 to 350 nm with 0.1 mM concentration of KCN, [Au(*cis*-DACH)Cl_2]Cl and [Au(*cis*-DACH)$_2$]Cl_3 in aqueous solution. In addition, kinetic measurements of these complexes with cyanide ion were prepared in aqueous solution.

^{1}H NMR measurements were carried out on a JEOL-LA 500 MHz NMR spectrophotometer at 297 K. The spectral conditions were 32 k data point, 3.2 s acquisition time, and 5.75 μs pulse width.

^{13}C NMR measurements were made at 125.65 MHz with ^{1}H broadband decoupling at 297 K. The spectral conditions were 32 k point data, 1 s acquisition time, 2.5 s pulse delay, and 5.12 μs pulse width. ^{15}N NMR measurements were obtained at 50.53 MHz at 297 K. The spectral conditions were 32 k data point, 0.8 s acquisition time, 10.0 s pulse delay, and 9.0 μs pulse width [28].

2.3. *Electrochemical technique*

A CHI660 potentiostat (http://www.chinstruments.com/) was used for all square wave voltammetric (SWV) measurements. The electrochemical cell contained a glassy carbon electrode (GCE; 3.0 mm diameter, Model CHI104, CH Instruments, Austin, TX) as a working electrode, Ag/AgCl (sat. KCl) reference electrode (Model CHI111, CH Instruments, Austin, TX), and a platinum wire counter electrode were inserted into a 2 mL glass cell through holes in its Teflon cover. Prior to each SWSV measurement, the GCE was polished with 3. 0 and 0.05 μm alumina slurries and washed with doubly distilled water. Each SWV measurement was performed at room temperature in a quiescent 0.2 M KCl aqueous solution, and with an initial potential of 0.0 V and final potential of +1.6 V.

2.4. *Synthesis of [Au(cis-DACH)Cl_2]Cl*

[Au(*cis*-DACH)Cl_2]Cl was synthesized according to the method described in the literature [18]. UV spectrum is 305 nm. ^{1}H NMR: 3.59, 2.02, 1.76, 1.47, and 1.29 m. ^{13}C NMR: 63.32, 26.83, and 21.42 ppm. Anal. Found (calculated) for $C_6H_{14}AuCl_3N_2$: C, 17.22 (17.26); H, (3.35) 3.38; N, 6.67(6.71).

2.5. *Synthesis of [Au(cis-DACH)$_2$]Cl_3*

[Au(*cis*-DACH)$_2$]Cl_3 was synthesized according to the method described in the literature [29]. UV spectrum is 344 nm. ^{1}H NMR: 3.58 m, 1.94 m, 1.74 m, 1.54 m, 1.38 m, and ^{13}C NMR: 61.75, 61.65, 26.37, 26.17, and 20.67 ppm. Anal. Found (calculated) for $C_{12}H_{28}AuCl_3N_4$: C, 27.02(27.11); H, 5.28(5.31); N, 10.61(10.54).

2.6. *Kinetic measurements*

The UV–vis spectra of the complex and cyanide solutions were recorded from 200 to 500 nm, figure 1 (five runs) shows λ max 305 and 258 nm for [Au(*cis*-DACH)Cl_2]Cl and [Au(*cis*-DACH)$_2$]Cl_3, respectively. The reactions were started by mixing the complex and

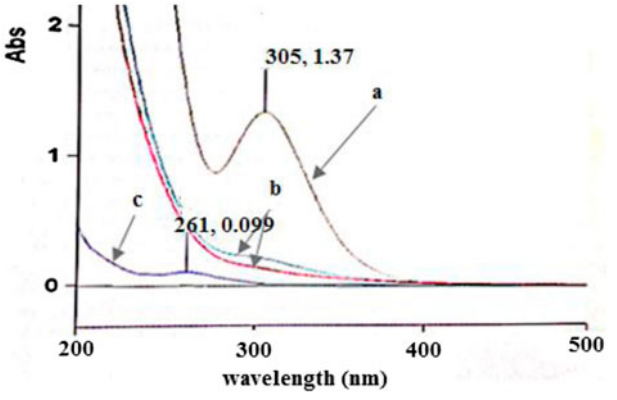

Figure 1. UV–vis spectra for [Au(*cis*-DACH)Cl_2]Cl (1.0×10^{-4} M) (a) before and (b) after addition of cyanide (5.0×10^{-3} M) and (c) cyanide before reaction, the substitution reaction carried out at ambient room temperature of 25 °C.

Table 1. Rate constant k, for substitution reaction of [Au(*cis*-DACH)Cl_2]Cl and [Au(*cis*-DACH)$_2$]Cl_3 with cyanide ion, in the presence of 20 mM NaCl in aqueous solution at 298 K.

λ max	[CN^-] (M)	k_{obsd} (s^{-1})	k_f (M^{-1} s^{-1})	k_b (M^{-1} s^{-1})	$\Delta H^{\neq}$ (kJ M^{-1})	$\Delta S^{\neq}$ (JK^{-1} M^{-1})	E_a (kJ M^{-1})
	[Au(DACH)Cl_2]Cl = 0.1 mM						
305 nm	0.00200	0.1993	148 ± 1.00	0.0011 ± 0.0001	39 ± 3.0	−80 ± 4.0	42 ± 4.0
	0.00300	0.3458					
	0.00400	0.5989					
	0.00500	0.7246					
	0.00600	0.9971					
	0.00800	1.3654					
	0.0100	1.7456					
	0.0200	2.8345					
	[Au(DACH)$_2$]Cl_3 = 0.1 mM						
258 nm	0.00200	0.0696	18 ± 1.0	0.0094 ± 1 × 0.0001	11 ± 2.0	− 185 ± 4.0	13 ± 2.0
	0.00300	0.0797					
	0.00400	0.09478					
	0.00500	0.10739					
	0.00600	0.11663					
	0.00800	0.14978					
	0.0100	0.2552					
	0.0200	0.38307					

cyanide solutions in equal volumes directly in a vial kept inside the instrument. The kinetic measurements were made under pseudo-first-order conditions, where concentration of the complex is 0.1 mM and for cyanide ranged from 2 to 10, 20 mM. The reactions were followed over 10 min and were carried out at 25 °C. The pseudo-first-order rate constant k_{obsd} is calculated as an average of eight independent kinetic runs (table 1). Observed experimental data are reported in table 1 [30]. The plots of pseudo-first-order rate constant of the reaction of these complexes with cyanide ion are shown in figures 2(A) and 2(B).

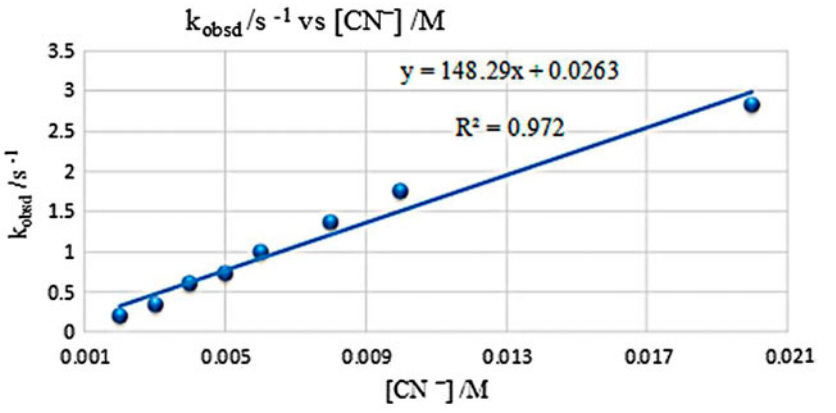

Figure 2(A). Plot of pseudo-first-order rate constant for the reaction between [Au(*cis*-DACH)Cl_2]Cl with cyanide in aqueous solution at 25 °C.

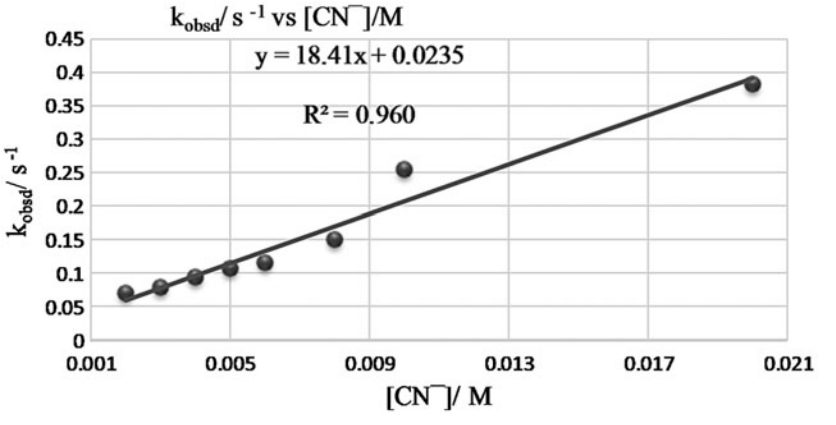

Figure 2(B). Plot of pseudo-first-order rate constant for the reaction between [Au(*cis*-DACH)$_2$]Cl_3 with cyanide in aqueous solution at 25 °C.

3. Results and discussion

3.1. *Interaction of [Au(cis-DACH)Cl_2]Cl with K^{13}CN*

Interaction of [Au(*cis*-DACH)Cl_2]Cl with enriched KCN was carried out in CH_3OD by mixing the reactants at different ratios and monitored by ^{1}H, ^{13}C, ^{15}N NMR, UV–vis spectroscopy, and electrochemistry. ^{1}H, ^{13}C, and ^{15}N NMR chemical shifts for the species in this interaction are given in tables 2–4(A) respectively.

When ^{13}C NMR is used to monitor the reaction [figure 3(a)], the chemical shift of (5 mM) 20% enriched K^{13}CN is at 160.48 ppm. The peak at 103 ppm [figure 3(b)] indicates the white precipitate [Au(^{13}CN)$_4$]$^-$. It is formed by interaction of [Au(*cis*-DACH)Cl_2]Cl with K^{13}CN at 1 : 0.25 equivalent, which is consistent with the peak that is monitored in previous studies [25, 27, 31]. [Au(^{13}CN)$_4$]$^-$ is not stable and goes through reductive

Table 2. ^{1}H NMR chemical shifts of the reaction of [Au(*cis*-DACH)(Cl_2]Cl with K^{13}CN ligand in CH_3OD solution.

	^{1}H (δ in ppm)				
Complex	H1, H2	H1, H2 eq	H3, H6 ex	H4, H5 eq	H4, H5 ex
(1 : 0)	3.59 m	2.02 m	1.76 m	1.47 m	1.29 m
(1 : 1)	3.56 m	2.00 m	1.75 m	1.48 m	–
(1 : 2)	3.39 m	1.87 m	1.62 m	1.40 m	0.86 m
(1 : 4)	3.61 m	1.76 m	1.51 m	1.32 m	0.86 m

Table 3. ^{13}C NMR chemical shifts of $^{13}CN^-$ for different species during the reaction of [Au(*cis*-DACH)Cl_2]Cl with cyanide in CH_3OD solution.

Complex	^{13}C (δ in ppm)	Refs.
KCN	160	[28]
[Au(DACH)(CN)Cl]Cl	101	This work
[Au(DACH)$(CN)_2$]Cl	96	This work
$[Au(CN)_4]^-$	103	[25–27]
$[Au(CN)_2Cl_2]^-$	119	[25]
HCN	137	This work
NCCN	110	[27]
[Au$(CN)_2$(OH)Cl]Cl	121	[25]
[Au$(CN)_2(OH)_2$]Cl	120	[25]
$[Au(CN)_2]^-$	152–157	[25–28]

elimination to form cyanogen (NCCN), which appeared at 110.52 ppm, while Au(III) was reduced to $[Au(^{13}CN)_2]^-$, which shifted downfield to 152–157 ppm, due to back donation of gold to cyanide [32]. $[Au(CN)_2]^-$ has higher stability due to its covalent bond than the corresponding $[Cu(CN)_2]^-$ and $[Ag(CN)_2]^-$ described by Wang *et al.* [33]. Figure 3(c) shows the ^{13}C spectrum, where peaks at 101.31 ppm and 95.50 ppm indicate the rapid exchange of consecutive chlorides by $^{13}CN^-$ to produce [Au(*cis*-DACH)(^{13}CN)Cl]$^-$ and $[Au(cis\text{-}DACH)(^{13}CN)_2]^-$, respectively. The downfield shift at 1 : 1.5 equivalent to 119.13, 120.52, and 121.34 ppm indicates formation of $[Au(CN)_2Cl_2]^-$, $[Au(CN)_3Cl]^-$, and [Au(^{13}CN)$_2$(OH)Cl]$^-$, respectively. The peak at 137 ppm indicates the HCN generated by 99.9% hydrolysis of K^{13}CN [27].

Table 4. (A)–(B) ^{15}N NMR chemical shifts of $^{13}C^{15}N^-$ for different species during reactions of [Au(*cis*-DACH)Cl_2]Cl **(A)** and [Au(*cis*-DACH)$_2$]Cl_3 **(B)** with K^{13}C^{15}N in CH_3OD and D_2O, respectively.

	^{15}N (δ in ppm)	
Complex	*A* (ppm)	*B* (ppm)
K^{13}C^{15}N	265.03	271.82
[Au(^{13}C^{15}N)$_2$]–	262.63	265.06
[Au(^{13}C^{15}N)$_4$]–	281.52	275.01

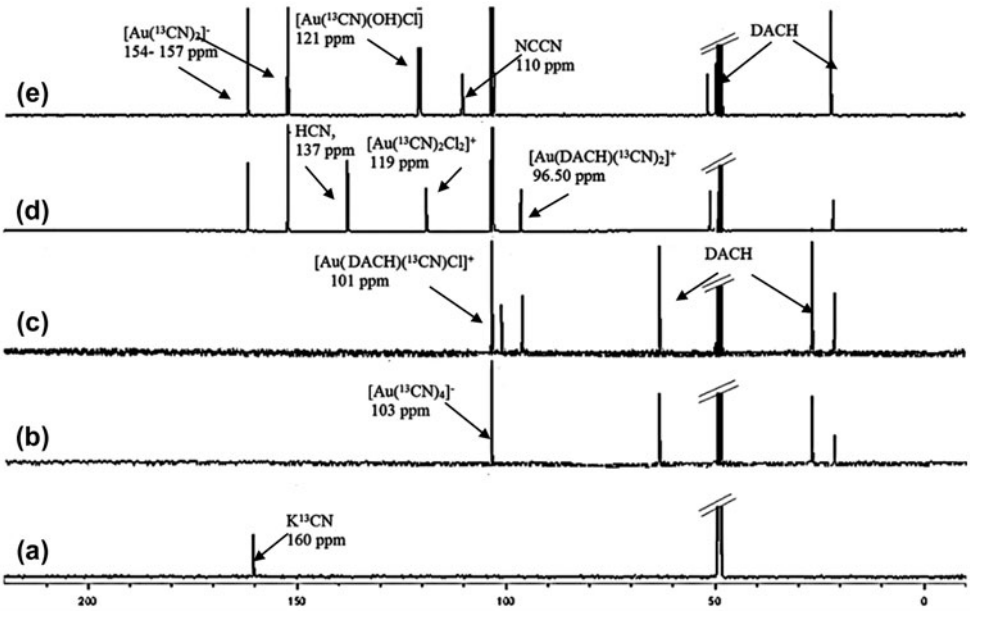

Figure 3. ^{13}C NMR spectra of (a) free $K^{13}CN$, (b) after reaction with [Au(*cis*-DACH)Cl_2]Cl at I : 0.25 ratio, (c) at 1 : 0.5 ratio, (d) at 1 : 1.5 ratio, and (e) at 1 : 2 ratio, in CH_3OD.

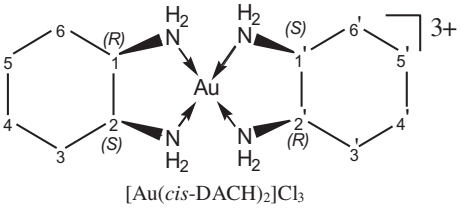

[Au(*cis*-DACH)$_2$]Cl_3

The ^{13}C spectrum, figure 3(d) sheds a light on reduction of $[Au(^{13}CN)_4]^-$ to $[Au(^{13}CN)_2]^-$ through intermediate complexes $[Au(^{13}CN)_2Cl_2]^-$, $[Au(^{13}CN)_3Cl]^-$, and [Au

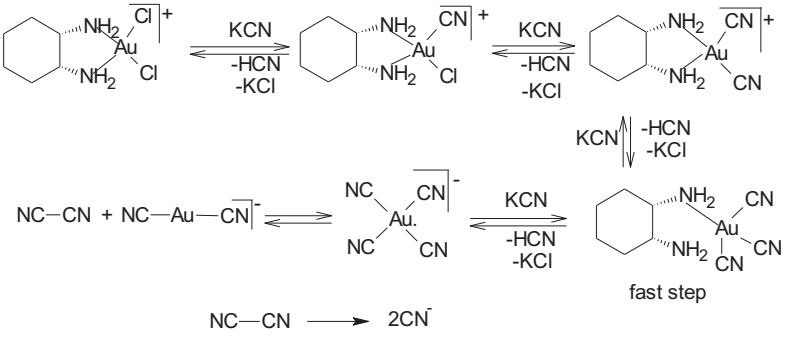

Scheme 1. Suggested mechanism for reaction of [Au(*cis*-DACH)Cl_2]Cl with $K^{13}CN$ in the range 1 : 0.25–1 : 4 equivalents.

$(^{13}CN)_2(OH)Cl]^-$ by displacement of cyanide by chloride through *cis* effect kinetics, unlike the behavior of Pt(II) described by Skibsted [34, 35].

The above mechanism is the solvolytic pathway through reversible exchange of chloride and H_2O.

The CN^- ion being the strong π-acceptor, and rapid exchange ligand removes DACH at 1 : 2 equivalents as shown via peaks at 53.03, 31.03, and 22.95 ppm [figure 3(e)] [26]. Table 2 shows ^1H NMR chemical shifts of [Au(*cis*-DACH)Cl_2]Cl interacting with CN^- at different equivalents. Figure S1a (see online supplemental material at http://dx.doi.org/10.1080/00958972.2014.971020) shows a peak at 265 ppm assigned to (5 mM) free 99.9% enriched $K^{13}C^{15}N$ and at 1 : 2 equivalent. This peak shifted downfield at 281 ppm assigned to $[Au(^{13}C^{15}N)_4]^-$ (figure S1b). At 1 : 4 equivalent (figure S1c), there are peaks at 262 and 281 ppm assigned to $[Au(^{13}C^{15}N)_2]^-$ and $[Au(^{13}C^{15}N)_4]^-$, respectively [36].

The obtained electrochemical results are in agreement with ^1H, ^{13}C, and ^{15}N NMR, and UV spectroscopy, and confirmed the suggested mechanism (scheme 1). Figure 4 and its inset show the SWVs obtained at the GCE in a quiescent aqueous solution of 0.2 M KCl. A well-defined SWV peak [figure 4(b)] was obtained at +0.82 V (*vs.* Ag/AgCl) for 1.0 mM [Au(*cis*-DACH)Cl_2]Cl. This peak showed a systematic decrease in peak area with subsequent additions of CN^- at different equivalents (1 : 0.5, 1 : 1, and 1 : 1.5) [figure 4(c)–(e)]. At 1 : 2 equivalents, peak disappearance was observed with appearance of a new shoulder at +1.4 V [figure 4(f)], which became more defined at 1 : 3 and 1 : 4 equivalents. Additions of CN^- to 0.2 M KCl solution in the absence of [Au(*cis*-DACH)Cl_2]Cl showed no peaks (data not shown).

3.2. *Interaction of [Au(cis-DACH)$_2$]Cl$_3$ with K^{13}CN*

Interaction of [Au(*cis*-DACH)$_2$]Cl_3 with 20% enriched $K^{13}CN$ was carried out in D_2O by mixing the reactants at different mole ratios and monitored by ^1H, ^{13}C, ^{15}N NMR, UV–vis spectroscopy, and electrochemistry. The ^1H, ^{13}C, and ^{15}N NMR chemical shifts for this interaction are given in tables 4(B) and 5. When ^{13}C NMR is used to monitor the interaction [figure 5(a)] a peak for (5 mM) 20% enriched $K^{13}CN$ is assigned at 157.44 ppm

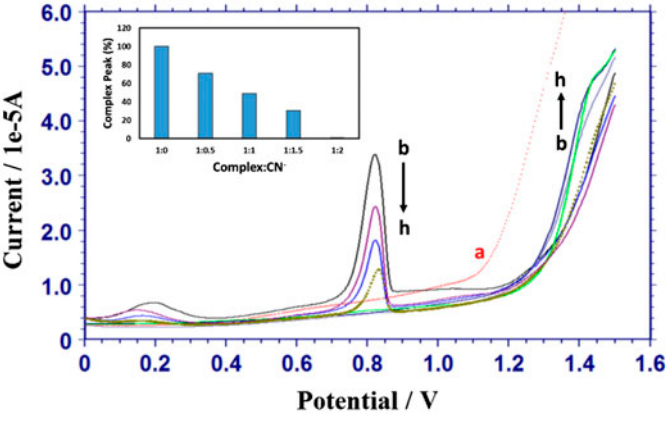

Figure 4. SWVs in 0.2 M KCl aqueous solution at a GCE in absence (a) and presence (b) of 1.0 mM [Au(*cis*-DACH)Cl_2]Cl, and subsequent additions of 0.5 mM (c)–(f) and 1.0 mM (g), (h) of KCN aqueous solution. Working conditions of the pulse width (increment), 4 mV; pulse height (amplitude), 25 mV; frequency, 15 Hz. Inset is the corresponding histogram at different complex: CN^- equivalents.

[figure 5(b)] and two new peaks upfield at 104.54 ppm and 119.87 ppm corresponding to $[Au(^{13}CN)_4]^-$ and $[Au(CN)_2Cl_2]^-$, respectively [25, 27]. When the reaction is carried out at 1 : 1 equivalent, the peak at 119.87 ppm shifts downfield (120.47 ppm) and a new peak is observed at 154.37 ppm, assigned to $[Au(^{13}CN)_2]^-$, the result of reductive elimination of $[Au(^{13}CN)_4]^-$ [figure 5(c)] [31].

Figure 5(d) shows a peak at 110.10 ppm of NCCN due to an oxidation of CN^- and reduction of Au(III) to Au(I) [27]. There is significant downfield shift of the 119.87 ppm resonance to 122.50 ppm corresponding to two very fast consecutive cyanide ligand exchanges by H_2O due to solvolytic pathway (scheme 2).

At higher concentration of $^{13}CN^-$ (1 : 4 equivalent) the upfield shift of DACH's carbons was observed, which corresponds to removal of *bis*-DACH ligands. The peak at 121 ppm is an indication of H_2O being exchanged by chloride to form $[Au(CN)_2(OH)Cl]^-$ [25].

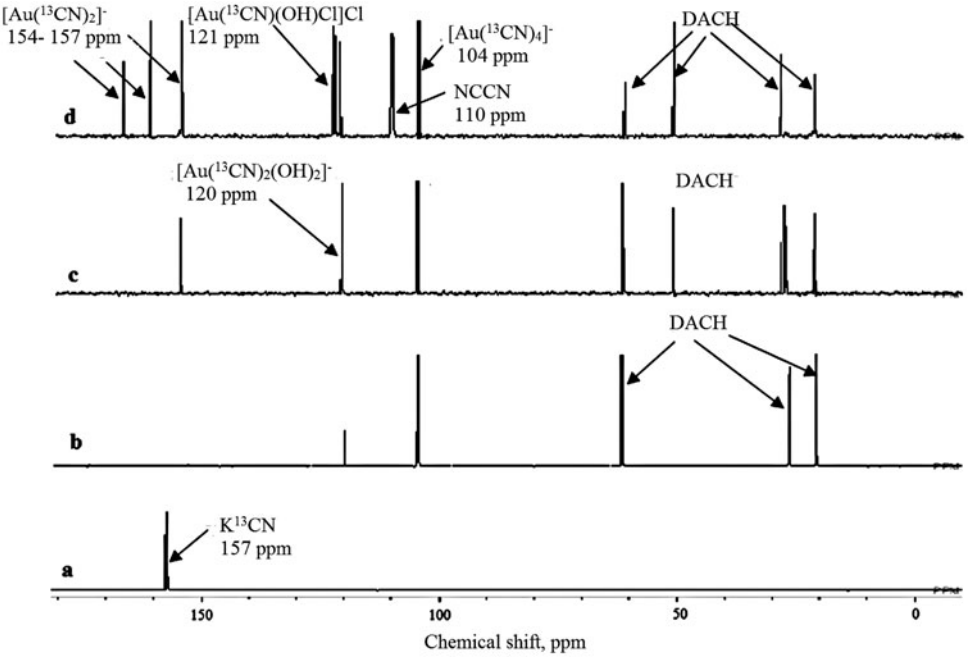

Figure 5. ^{13}C NMR spectra of (a) free $K^{13}CN$, (b) after reaction with $[Au(cis\text{-}DACH)_2]Cl_3$ at I : 0.25 ratio, (c) at 1 : 1 ratio, (d) at 1 : 2 ratio in D.

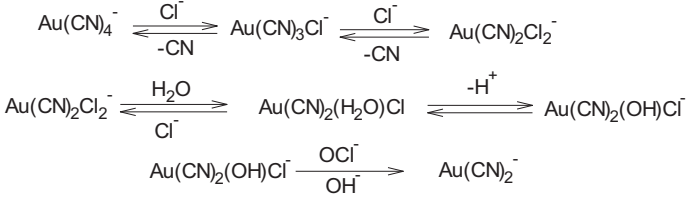

Scheme 2. A suggested mechanism of conversion $[Au(^{13}CN)_4]^-$ to $[Au(^{13}CN)_2]^-$.

Table 5 shows ^{1}H NMR chemical shifts for [Au(*cis*-DACH)$_2$]Cl$_3$ reaction with K^{13}CN from 1 : 1 to 1 : 4 equivalents that confirmed the ^{13}C NMR interpretation.

Figure S2a shows the ^{15}N NMR spectra for the reaction with (50 mM) 99.9% enriched K^{13}C^{15}N at 271 ppm. Figure S2b shows two peaks at 275.01 ppm and 265.06 ppm assigned for [Au(^{13}C^{15}N)$_4$]$^-$ and [Au(^{13}C^{15}N)$_2$]$^-$, respectively.

Figure S3 shows a SWV peak for [Au(*cis*-DACH)$_2$]Cl$_3$ at +1.35 V (*versus* Ag/AgCl). The peak area of the obtained peak was decreased systematically with equivalent additions of CN$^-$. However, due to the relatively high potential (+1.35 V), the decrease was not easy to follow, yet the trend is there.

3.3. *Kinetic data*

The substitution reactions of these square-planar gold(III) complexes [Au(*cis*-DACH)Cl$_2$]Cl and [Au(*cis*-DACH)$_2$]Cl$_3$ with cyanide were investigated spectrophotometrically by the change of absorbance at selected wavelengths as function of time under pseudo-first-order conditions. The substitution reaction proceeds through an associative mechanism. All reactions were studied in aqueous solution. Addition of 20 mM NaCl prevents hydrolysis of the complex. The suggested reaction mechanism of cyanide with [Au(*cis*-DACH)Cl$_2$]Cl is shown in scheme 1. The rate constants are determined from plots of linear dependence of k_{obsd} *versus* total cyanide concentration [figure 2(A)] according to equation (1). The slope of the line represents k_f, while the intercept indicates k_b [Cl$^-$]. All kinetic data are summarized in table 1.

$$K_{obsd} = k_f\ [CN^-] + k_b\ [Cl^-] \tag{1}$$

The enthalpy, entropy, and activation energies for the reaction of [Au(*cis*-DACH)Cl$_2$]Cl with cyanide are calculated using the Eyring and Arrhenius equations. From the rate constant values, [Au(*cis*-DACH)Cl$_2$]Cl reacts much faster than [Au(*cis*-DACH)$_2$]Cl$_3$. The difference in reactivity can be attributed to the presence of two (*cis*-DACH) ligands, leading to decrease in electrophilicity of the gold center, due to electron density delocalization through the π-back bonding effect [37].

The reactivity of the cyanide ligand is much greater than the following nucleophiles: L-histidine (L-His), guanine-5′-monophosphate (5′-GMP), inosine (Ino), and inosine-5′-monophosphate (5′-IMP) toward [Au*(cis*-DACH)Cl$_2$]Cl [30, 38].

Table 5. ^{1}H NMR chemical shifts of DACH protons for the reaction of [Au(*cis*-DACH)$_2$]Cl$_3$ with (K^{13}CN) in D$_2$O solution.

	^{1}H (δ in ppm)				
Complex	H1, H2	H3, H6 eq.	H3, H6 ex.	H4, H5 eq.	H4, H5 ex.
(1 : 0)	3.58 m	1.94 m	1.74 m	1.56 m	1.38 m
(1 : 1)	3.32, 3.20 m	1.86 m	1.65 m	1.53 m	1.33 m
(1 : 2)	3.21, 3.06 m	1.80 m	1.62 m	1.49 m	1.26 m
(1 : 4)	3.75, 2.85 m	–	1.65 m	1.42 m	1.23 m

Table 6. Rate constants for substitution of [Au(*cis*-DACH)Cl_2]Cl and [Au(*cis*-DACH)$_2$]Cl_3 with cyanide in the presence of 20 mM NaCl in aqueous solution at 298 K.

	k_f (M^{-1} s^{-1})	K_b (M^{-1} s^{-1})	$\Delta H^{\neq}$ (kJ M^{-1})	$\Delta S^{\neq}$ (JK^{-1} M^{-1})	ΔE_a (kJM^{-1})	Refs.
[Au(*cis*-DCH)Cl_2]$^+$						
Cyanide	148 ± 3.00	0.0011 ± 0.0001	39 ± 3.0	−80 ± 4.0	42 ± 4.0	This work
L-His	75 ± 2	4.00 ± 0.1	12 ± 3	−160 ± 10	–	[30]
5′-GMP	66 ± 2	9.3 ± 0.20	10 ± 3	−180 ± 10	–	[30, 38]
5′-IMP	6.0 ± 0.3	0.20 ± 0.010	–	–	–	[30]
Ino	9.9 ± 0.9	0.060 ± 0.020	–	–	–	[30]
[Au(*cis*-DACH)$_2$]$^{3+}$						
Cyanide	18 ± 1.0	0.0094 ± 0.0001	11 ± 2.0	−185 ± 4.0	13 ± 2.0	This work
L-His	–	–	–	–	–	–
5′-GMP	–	–	–	–	–	–
5′-IMP	–	–	–	–	–	–
Ino	–	–	–	–	–	–

The reactivity order of these ligands toward [Au(*cis*-DACH)Cl_2]Cl is CN^- >>> L-His > 5′-GMP > Ino > 5′-IMP (table 6). Its substitution reaction and absorption around 305 nm are shown in figure S4, with a SWV peak at +0.82 V as shown in figure 4, whereas [Au(*cis*-DACH)$_2$]Cl_3 is around 344 nm with SWV peak at +1.35 V as shown in figure S3.

Figure S5 shows UV spectra of an oxidation reduction reaction of [Au(*cis*-DACH)Cl_2]Cl with CN^- ion at (complex : ligand) 1 : 2 equivalent. The bands at 204 nm and 211 nm correspond to $[Au(CN)_2]^-$ by back donation from d orbital(d^8) in Au(III) to empty π*-acceptor in cyanide ligand, which strengthens Au–CN and weakens Au–NR. Figure S6 shows an oxidation reduction reaction of [Au(*cis*-DACH)Cl_2]Cl with CN^- ion at 1 : 4 equivalent. The bands observed at 204, 211, and 240 nm which are assigned to $[Au(CN)_2]^-$ that remains unchanged after 24 h indicate complete oxidation reduction reaction [39, 40]. Figures 6(A) and (B) show pseudo-first-order rate constant as function of nucleophilic concentration and temperature for reaction of [Au(*cis*-DACH)Cl_2]Cl and [Au(*cis*-DACH)$_2$]Cl_3 with cyanide.

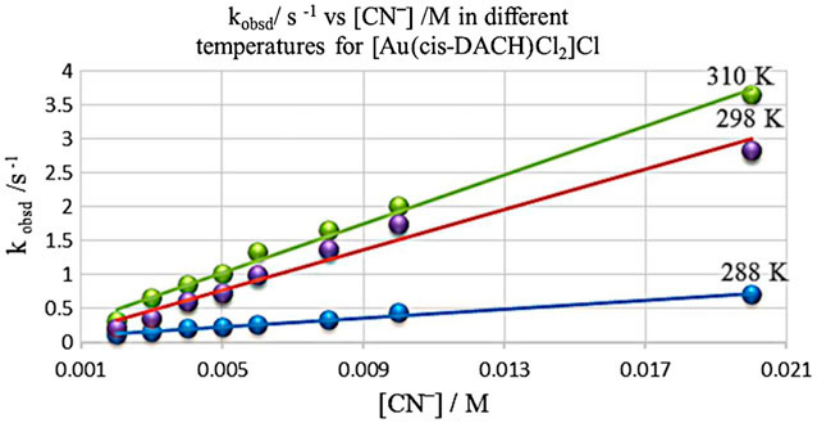

Figure 6(A). Plot of pseudo-first-order rate constants as a function of nucleophilic concentration and temperature for the reaction between [Au(*cis*-DACH)Cl_2]Cl and cyanide in the presence of 20 mM NaCl in aqueous solution.

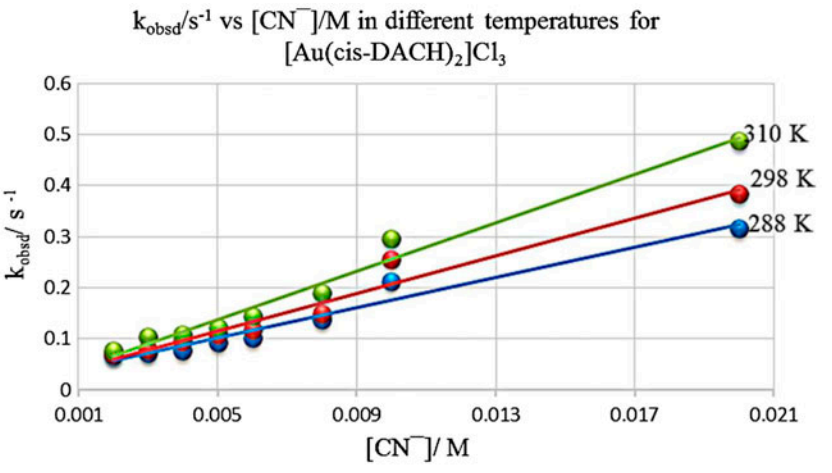

Figure 6(B). Plot of pseudo-first-order rate constants as a function of nucleophilic concentration and temperature for the reaction between $[Au(cis\text{-}DACH)_2]Cl_3$ and cyanide in the presence of 20 mM NaCl in aqueous solution.

4. Conclusion

This work describes NMR spectroscopy, electrochemistry, and kinetic studies of the reaction mechanism of $[Au(cis\text{-}DACH)Cl_2]Cl$ and $[Au(cis\text{-}DACH)_2]Cl_3$ with cyanide in aqueous and methanolic solutions. $[Au(cis\text{-}DACH)Cl_2]Cl$ shows faster reaction toward cyanide than $[Au(cis\text{-}DACH)_2]Cl_3$. At 1 : 0.25 equivalent of $[Au(cis\text{-}DACH)_2]Cl_3$ with $K^{13}CN$, there are two complexes formed corresponding to $[Au(^{13}CN)_4]^-$ and $[Au(^{13}CN)_2Cl_2]^-$. While at the same equivalent of KCN with $[Au(cis\text{-}DACH)Cl_2]Cl$, only one complex formed corresponding to $[Au(^{13}CN)_4]^-$. At 0.75 equivalent of $K^{13}CN$ added to solution of $[Au(cis\text{-}DACH)_2]Cl_3$, the formed $[Au(^{13}CN)_4]^-$ reduces to $[Au(^{13}CN)_2]^-$. Whereas the same equivalent of $K^{13}CN$ added to $[(cis\text{-}DACH)AuCl_2]Cl$, the reaction proceeds through two consecutive cyanide exchanges to produce $[Au(cis\text{-}DACH)(^{13}CN)Cl]^-$ and $[Au(cis\text{-}DACH)(^{13}CN)_2]^-$ along with $[Au(^{13}CN)_4]^-$. Kinetically, $[Au(cis\text{-}DACH)Cl_2]Cl$ reacts much faster than $[Au(cis\text{-}DACH)_2]Cl_3$ with KCN. These results may contribute to a better understanding of biochemical mechanism of $[Au(cis\text{-}DACH)Cl_2]Cl$ and $[Au(cis\text{-}DACH)_2]Cl_3$.

Acknowledgement

This research was supported by the KFUPM Research Committee under DSR project # IN121049.

References

[1] V. Volarevic, M. Milovanovic, A. Djekovic, Ž.D. Bugarcic, N. Arsenijevic. *Ser. J. Exp. Clin. Res.*, **13**, 99 (2012).
[2] D. Fan, C.T. Yang, J.D. Ranford, J.J. Vittal. *Dalton Trans.*, **24**, 4749 (2003).
[3] M. Bortoluzzi, A. Scrivanti, A. Reolon, E. Amadio, V. Bertolasi. *Inorg. Chem. Commun.*, **33**, 82 (2013).
[4] S.L. Best, Z. Guo, M.I. Djuran, P.J. Sadler. *Met. Based Drugs*, **6**, 261 (1999).

[5] I. Ott. *Coord. Chem. Rev.*, **253**, 1670 (2009).
[6] N. Pantelić, B.B. Zmejkovski, J. Trifunović-Macedoljan, A. Savić, D. Stanković, A. Damjanović, Z. Juranić, G.N. Kaluđerović, T.J. Sabo. *J. Inorg. Biochem.*, **128**, 146 (2013).
[7] J.J. Zhang, W. Lu, R.W. Sun, C.M. Che. *Angew. Chem. Int. Ed.*, **51**, 4882 (2012).
[8] M. Serratrice, M.A. Cinellu, L. Maiore, M. Pilo, A. Zucca, C. Gabbiani, A. Guerri, I. Landini, S. Nobili, E. Mini, L. Messori. *Inorg. Chem.*, **51**, 3161 (2012).
[9] L. Messori, G. Marcon, P. Orioli. *Bioinorg. Chem. Appl.*, **l**, 177 (2003).
[10] P.C. Hydes, M.J.H. Russell. *Cancer Metast. Rev.*, **7**, 67 (1988).
[11] L. Maiore, M.A. Cinellu, S. Nobili, I. Landini, E. Mini, C. Gabbiani, L. Messori. *J. Inorg. Biochem.*, **108**, 123 (2012).
[12] C. Gabbiani, A. Guerri, M.A. Cinellu, L. Messori. *Open Crystallogr. J.*, **3**, 29 (2010).
[13] J.F. Vollano, S. Al-Baker, J.C. Dabrowiak, J.E. Schurig. *J. Med. Chem.*, **30**, 716 (1987).
[14] B.A. Al-Maythalony, A.A. Isab, M.I. Wazeer, A. Ibdah. *Inorg. Chim. Acta*, **363**, 3200 (2010).
[15] S. Zhu, W. Gorski, D.R. Powell, J.A. Walmsley. *Inorg. Chem.*, **45**, 2688 (2006).
[16] C.D. Sanghvi, P.M. Olsen, C. Elix, S. Peng, D. Wang, Z. Chen, D.M. Shin, K.I. Hardcastle, C.E. MacBeth, J.F. Eichler. *J. Inorg. Biochem.*, **128**, 68 (2013).
[17] A. Ahmed, D.M. Al Tamimi, A.A. Isab, A.M. Alkhawajah, M.A. Shawarby. *PLoS ONE*, **7**, e51889 (2012).
[18] S.S. Al-Jaroudi, M. Fettouhi, M.I. Wazeer, A.A. Isab, S. Altuwaijri. *Polyhedron*, **50**, 434 (2013).
[19] M. Monim-ul-Mehboob, M. Altaf, M. Fettouhi, A.A. Isab, M.I.M. Wazeer, M. Shaikh, S. Altuwaijri. *Polyhedron*, **61**, 225 (2013).
[20] A.A. Isab, S. Ahmad. *J. Spectroscopy*, **20**, 109 (2006).
[21] C.F. Shaw III, S. Schraa, E. Gleichmann, Y.P. Grover, L. Dunemann, A. Jagarlamudi. *Met. Based Drugs*, **1**, 351 (1994).
[22] M.A. Rawashdeh-Omary, M.A. Omary, H.H. Patterson. *J. Am. Chem. Soc.*, **122**, 10371 (2000).
[23] A.A. Isab, S. Ahmad, W. Ashraf. *Transition Met. Chem.*, **30**, 389 (2005).
[24] S.D. Khanye, G.S. Smith, C. Lategan, P.J. Smith, J. Gut, P.J. Rosenthal, K. Chibale. *J. Inorg. Biochem.*, **104**, 1079 (2010).
[25] A.J. Canumalla, N. Al-Zamil, M. Phillips, A.A. Isab, C.F. Shaw III. *J. Inorg. Biochem.*, **85**, 67 (2001).
[26] P.M. Yangyuoru, J.W. Webb, C.F. Shaw. *J. Inorg. Biochem.*, **102**, 584 (2008).
[27] B.A. Al-Maythalony, M.I. Wazeer, A.A. Isab. *Inorg. Chim. Acta*, **363**, 3244 (2010).
[28] S. Ahmad, A.A. Isab, A.R. Al-Arfaj, A.P. Arnold. *Polyhedron*, **21**, 2099 (2002).
[29] S.S. Al-Jaroudi, M. Monim-ul-Mehboob, M. Altaf, M. Fettouhi, M.I.M. Wazeer, S. Altuwaijri, A.A. Isab. *New J. Chem.*, **38**, 3199 (2014). doi:10.1039/c3nj01624b.
[30] A. Djeković, B. Petrović, Živadin D. Bugarčić, R. Puchta, R. van Eldik. *Dalton Trans.*, **41**, 3633 (2012).
[31] K.J. Harris, R.E. Wasylishen. *Inorg. Chem.*, **48**, 2316 (2009).
[32] R. Crabtree. *The Organometallic Chemistry of The Transition Metals*, 5th Edn, p. 164, Wiley & Sons, New Jersey (2009).
[33] X.B. Wang, Y.L. Wang, J. Yang, X.-P. Xing, J. Li, L.S. Wang. *J. Am. Chem. Soc.*, **131**, 16368 (2009).
[34] L.H. Skibsted. In *Advances in Inorganic and Bioinorganic Mechanism*, A.G. Sykes (Ed.), Vol. 4, p. 137, Academic Press, New York, NY (1986).
[35] R. Pearson, F. Basolo. Mechanisms of Inorganic Reactions, 2nd Edn, Vols. 139–141, pp. 410–414, Wiley & Sons, New York (1967).
[36] M.N. Akhtar, A.A. Isab, A.R. Al-Arfaj. *J. Inorg. Biochem.*, **66**, 197 (1997).
[37] M. Bortoluzzi, G. Paolucci, B. Pitteri. *Polyhedron*, **29**, 767 (2010).
[38] M. Arsenijevic, M. Milovanovic, V. Volarevic, A. Djekovic, T. Kanjevac, N. Arsenijevic, Svetlana Dukic, Z.D. D. Bugarcic. *Med. Chem.*, **8**, 2 (2012).
[39] W.R. Mason III, H.B. Gray. *Inorg. Chem.*, **7**, 55 (1968).
[40] M.A. Ivanov, M.V. Puzyk, K.P. Balashev. *Russ. J. Gen. Chem.*, **76**, 881 (2006).